Aeroelastic model test of a 610 m-high TV tower with complex shape and structure

Quanshun Ding[1,2] and Ledong Zhu[*1,2]

[1]*State Key Laboratory of Disaster Reduction in Civil Engineering, Tongji University, Shanghai 200092, China*
[2]*Department of Bridge Engineering, College of Civil Engineering, Tongji University, Shanghai 200092, China*

Abstract. In view of the importance of the wind-structure interaction for tall and slender structures, an aeroelastic model test of the 610m-high TV tower with a complex and unique structural configuration and appearance carried out successfully. The assembled aeroelastic model of the TV tower with complex shape and structure was designed and made to ensure the similarities of the major natural frequencies and the corresponding mode shapes. The simulation of the atmospheric boundary layer with higher turbulent intensity is presented. Since the displacement and acceleration responses at several measurement sections were directly measured in the wind tunnel test, a multi-mode approach was presented to indirectly estimate the displacement and acceleration responses at arbitrary structural floors based on the measured ones. It can be seen that it is remarkable for the displacement and acceleration responses of the TV tower in the two horizontal directions under wind loads and is small for the dynamic response of the torsional displacement and acceleration.

Keywords: TV tower; wind tunnel test; aeroelastic model; simulation of atmospheric boundary layer; displacement response; acceleration response

1. Introduction

Wind loads are the most important loads controlling the design of high-rise structures, especially of those located in strong wind-prone regions, such as the east and south coastal regions of China. In the early 1960s, Davenport (1961a,b) pioneered the application of the statistical concepts of the stationary time history and the stochastic vibration theory to analyzing wind-induced vibrations of structures in conjunction with the quasi-steady theory because of the stochastic behavior of the natural wind. Through half-century efforts made by researchers in the world, significant progresses have been made on the theory and the technique of wind tunnel test for predicting the wind-induced responses of structures. The wind tunnel tests of aerodynamic model and of aeroelastic model (Boggs and Peterka 1989, Wang 1998, Fediw *et al*. 1995, Quan 1999), and the semi-theoretical analysis based on necessary aerodynamic parameters obtained via wind tunnel tests are often employed for the prediction of wind-induced static/dynamic responses of structures (Kareem 1992, Solari 1993, Zhou *et al*. 2000, Bienkiewicz *et al*. 1995, Kikuchi *et al*.

∗Corresponding author, Professor, E-mail: ledong@tongji.edu.cn

1997, Baker 2000, Carassale *et al*. 2001). However, the structural responses to winds are often investigated separately in along-wind direction and cross-wind direction (Zhou *et al*. 1999a,b, Ye 2000, Kwok 1982). The along-wind response is generally analyzed under the quasi-steady frame whilst the cross-wind response has more complicated mechanism and there is no mature and widely-acceptable analytical approach. This kind of traditional research way will be inadequate to spatial and asymmetric structures because of strongly coupled effects between vibrations in different directions and between different modes often occur in this case. Moreover, for accurate estimation of the acceleration response, it is important to consider not only the first two lateral vibrational modes, but also higher modes (Aly 2014).

Aerodynamic model test includes two major kinds, i.e., measurement of dynamic forces using high-frequency force balance and simultaneous measurements of wind pressures at multi-positions on building surface (Liang *et al*. 2004, Gu *et al*. 2004, Rosa *et al*. 2012, Tanaka *et al*. 2012, Aly 2013). Only wind environment and building shape are simulated in this kind of win tunnel tests, and the structural dynamic properties are not simulated when using rigid models. Therefore, the aeroelastic effect, i.e., the interaction between wind and structural motion, cannot be included in such tests and in the theoretical analysis based on the aerodynamic loads obtained via this kind of tests. Furthermore, linear mode shape has to be assumed in the analyses of wind-induced vibrations based on the results of high-frequency force balance test with rigid models. This leads to certain errors although some techniques for mode shape corrections have been proposed (Xu and Kwok 1993, Zhou *et al*. 2002).

However, it is noted that the effect of aerodynamic damping which could be positive or negative is very important to some high-rise buildings. To simulate the interaction between wind and structural motion, the dynamic properties of structures should be simulated in an aeroelastic model test besides the wind environment and the structural shape (Quan 1999). There are also two major kinds of aeroelastic model test. One is called the test of lump mass or multi-DOF aeroelastic model, and another is called the test of elasticly-supported rigid model or single-DOF model. The former can consider the multi-mode effect and has thus higher accuracy. However, it is more difficult and complicated in the model design and manufacture, and needs long time period and more expense. The latter is relatively simple in the model design and manufacture, and merely needs lower expense, however, it can only simulate one mode in each direction with the assumption of linear mode shape, thus has lower accuracy. Motion effects on the aerodynamic forces for an oscillating tower are investigated by Diana *et al*. (2009) through wind tunnel tests. To investigate the effect of tapering on reducing the rms across-wind displacement responses of a tall building, an experiment using an aeroelastic tapered model of a tall building was conducted in a wind tunnel which simulated the suburban environment (Pozzuoli *et al*. 2013). A wide experimental campaign was carried out in this study in order to evaluate the wind-induced loads and responses of a continuous equivalent aeroelastic model of a regular square-section tall building (Kim *et al*. 2008). Giappino *et al*. (2015) performed an aerodynamic and aeroelastic experimental study on sectional and simplified three-dimensional models of rectangular tall building, which both a rigid and a moving model of the building were tested to analyze possible aeroelastic effects. Obviously, the foregoing methods for the prediction of wind-induced responses of high-rise structures have their own advantages and disadvantages. Therefore, the research methods adopted in practice should be determined according to the characteristics of the structure concerned and research conditions available.

2. Guangzhou new TV tower

As shown in Fig. 1, Guangzhou New TV Tower is located at the south bank of Pear River in Guangzhou City in the south of China and on the new central line of the City. The 610 m high TV tower, including a main structure 460 m-high above the ground and a 150 m-high steel antenna mast, is one of the tallest TV towers in the world. Its main structure is comprised of a reinforced-concrete inner core canister serving as a routeway of vertical transportation, five vertically-arranged closed functional regions connected to the inner core eccentrically at unequal interval spaces, and an outer frame canister of twisted waist-drum shape composed of 24 inclined columns of concrete-filled steel tubes with diameters between 2.0 m (at -10.0 m elevation) and 0.9 m (at +450.0 m elevation) and oblique web tubes. The inner core canister has an elliptic horizontal cross-section with a constant inside long-axis of 18 m and a constant inside short-axis of 15 m and a thickness of about 0.3 m. The outer frame canister has varying and rotating elliptic horizontal cross-sections along height. The long-axes at bottom, waist and top are 80 m, 35.3 m and 54 m, respectively. The short-axes at bottom, waist and top are 60 m, 20.3 m and 40.5 m, respectively. The closed functional regions between the inner core canister and the outer frame canister have also varying elliptic horizontal cross-sections.

(a) Imaginary view   (b) Vertical section   (c) Typical horizontal sections
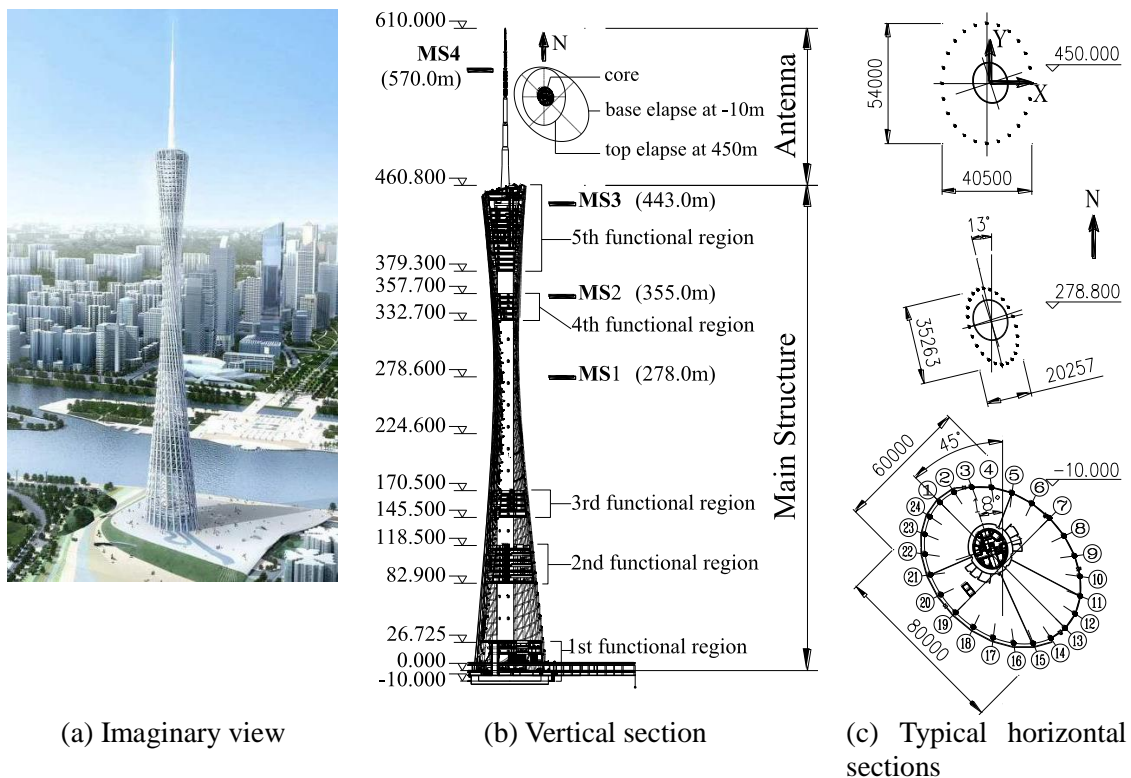
Fig. 1 Guangzhou New TV tower

Obviously, the TV tower shows strong spatial and asymmetric characteristics in structure, which will lead a dynamic behavior of multi-directional and multi-mode coupled vibration. With the natural frequency of fundamental bending mode being only 0.095Hz, the TV tower is a very flexible high-rise structure, and is thus susceptible to wind. Furthermore, the TV tower is located in a strong typhoon-prone region in the south of China, wind loads were therefore the most important loads controlling the structural design. Thus, comprehensive wind tunnel tests and analysis of wind-induced vibration were carried out to check the wind-resistant performance and to determine the static and dynamic wind-induced loads for the safe design of the TV tower with such uniqueness in both structural configuration and appearance. This paper mainly focuses on the relevant information and major results of the wind tunnel test of full tower aeroelastic model.

3. Aeroelastic model

The wind tunnel test of full tower aeroelastic model of Guangzhou New TV Tower was carried out in TJ-2 Boundary Layer Wind Tunnel at Tongji University. The testing section of the wind tunnel is 3 m wide, 2.5 m high and 15 m long, and the range of wind speed is 1 to 68 m/s. The geometric length scale λ_L was selected as 1:266, according to the dimensions of the wind tunnel and the TV tower. Because of little influence of the gravity on the stiffness of such a high-rise structure, the simulation of Froude Number was not considered in the model design. Thus, the frequency scale λ_f was set to be 47:1 to facilitate the manufacture of model and to have an adequate range of testing wind speed as well. The velocity scale λ_V was thus 1:5.66. The density scale $\lambda_\rho = 1$ is unchangeable because the air in the field is same as that in the wind tunnel. Therefore, the other scales were derived from the three basic scales of λ_f, λ_L and λ_ρ through dimensional analysis.

Because it is almost impossible to simulate directly the stiffness of individual small structural members at a length scale of 1:266, the effective bending and torsional stiffness of the entire structure and the distribution of mass and inertial moment of mass about vertical axis were simulated to ensure the similarities of the major natural frequencies and the corresponding mode shapes. To this end, the aeroelastic model was designed to consist of a steel core column with varying cross-section along the height, some divided coat segments and proper compensating weights. The steel core column was comprised of a lower part and an upper part used to simulate the stiffness of the main structure and the antenna mast, respectively. The stiffness parameters of the steel core column were derived inversely at first from the distribution information of mass and inertial moment of mass, the frequencies and mode shapes of the entire structure vibration and the mast-dominant vibration. As a result, the steel core column of the main structure model, which was placed on the central line of the elliptic inner core canister, was of a flute steel bar with six kinds of cross-sections and its major axes were consistent with the resultant vibration directions of the corresponding natural modes of the entire structure. The core column of the antenna mast model, which was placed on the central line of the mast, was of a steel thin-wall box bar with seven kinds of cross-sections and its major axes were consistent with the resultant directions of the corresponding natural modes of the antenna mast.

The coats of the main structure model were composed of ten inner-layer coat segments and eleven outer-layer coat segments. The inner-layer coat segments were made of perspex plates shaped via hot-pressing to simulate the shapes of the reinforced-concrete inner core canister and

the closed functional regions. The outer-layer coat segments were made through gluing together small perspex tubes of various diameters, and were used to simulate the shape of the outer frame canister. Some perspex tubes were carefully wrapped with paper adhesive tapes to meet the similarity requirement of diameter. During the assembly of the model, the inner-layer coat segments were firstly mounted on the steel core using some screws and the outer-layer coat segments were then connected to the inner-layer coat segments using some connectors of perspex tubes. The mast shapes of the lower four truss segments were simulated with four coat segments made of thin steel wires welded together, whilst those of the upper three segments were simulated with the steel-box core bars directly.

Because the steel core column of the main structure took a rather big portion of mass but provided a little portion of inertia moment of mass, the simulation of inertia moment of mass were fulfilled through fixing some compensating weights of lead bars on the walls of the inner-layer coats and putting proper lead wires into the tubes of outer-layer coats.

Fig. 2 shows the aeroelastic model of the TV tower mounted in TJ-2 Wind Tunnel. The model was rigidly fixed at the center of a turntable with a diameter of 2.8 m. Models of surrounding buildings located in a circular region with a radius of 500 m were made of ABS plastic plates at the same scale. Those models of surrounding buildings within a circular region with a radius of 372 m ($\approx 0.5 \times 2.8 \times 266$) were fixed on the turntable together at the corresponding right positions relative to the TV tower model, whilst the others were mounted on the windward tunnel floor at the corresponding right positions only when they were located at windward positions relative to the TV tower model. Hence, when the wind direction was changed during the test, the surrounding models on the turntable moved automatically with the rotation of the turntable, but those out of the turntable had to be moved manually to the desired locations.
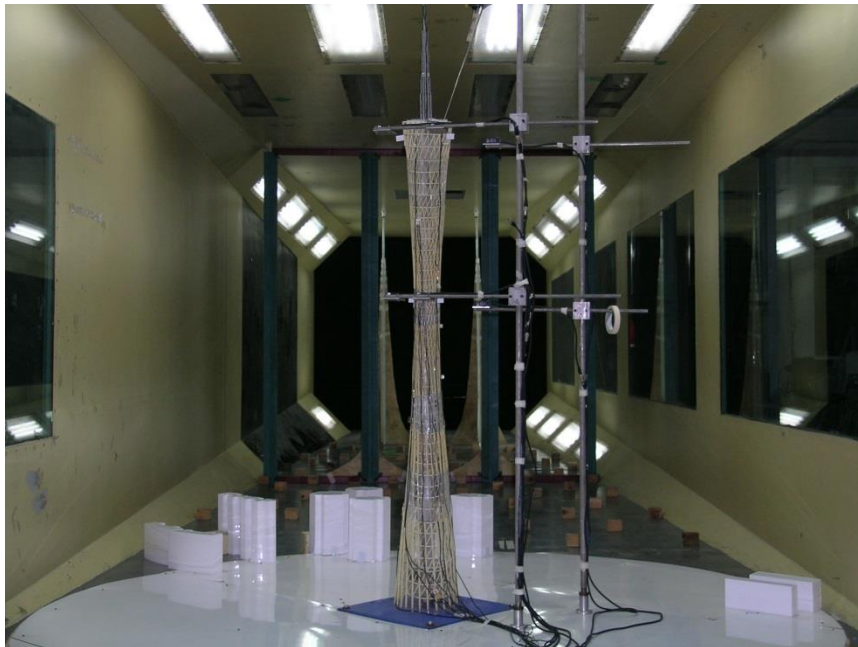

Fig. 2 Full tower aeroelastic model of the TV tower in the TJ-2 wind tunnel
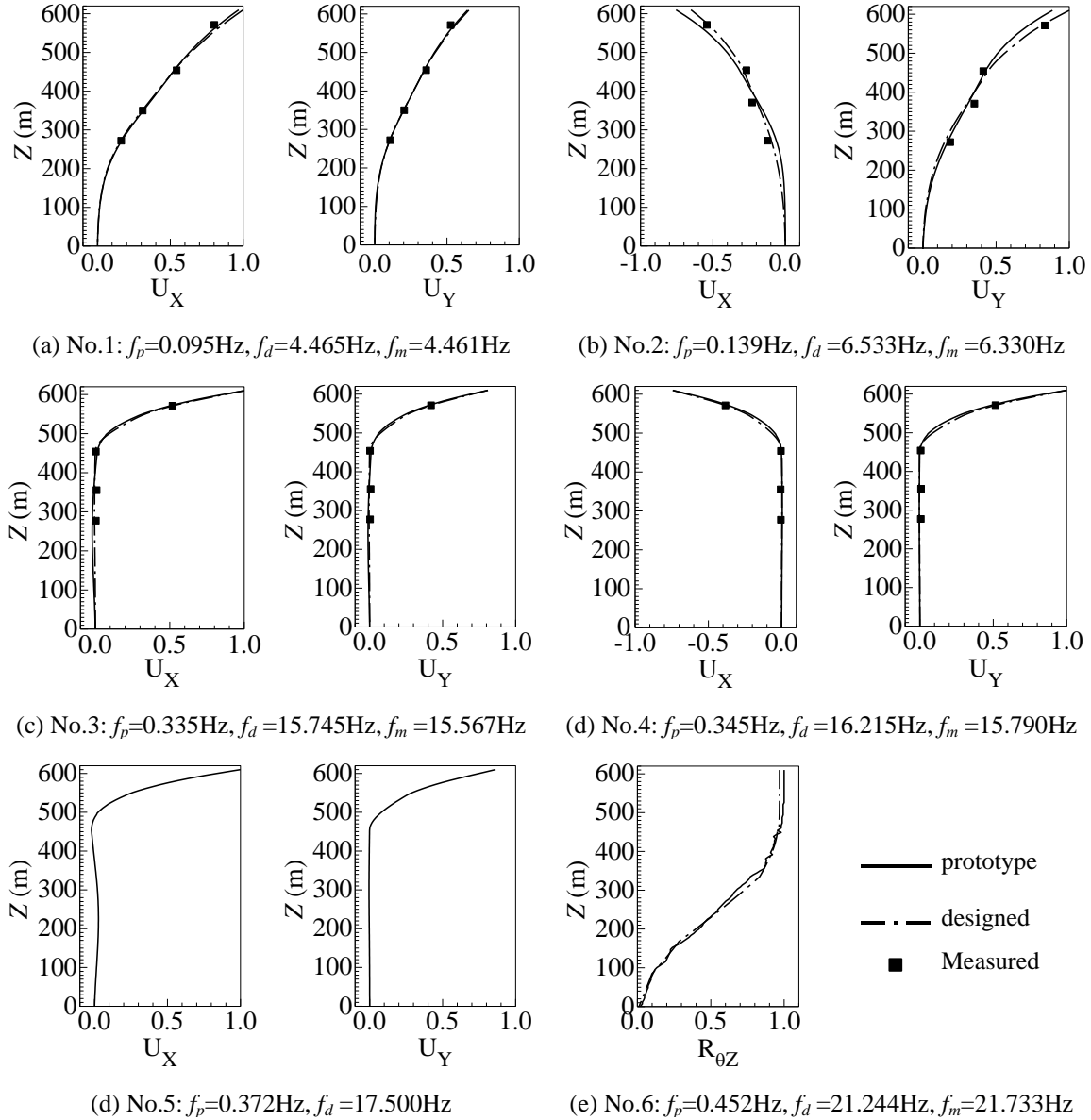
4. Check of modal parameters

(a) No.1: f_p=0.095Hz, f_d=4.465Hz, f_m=4.461Hz

(b) No.2: f_p=0.139Hz, f_d=6.533Hz, f_m=6.330Hz

(c) No.3: f_p=0.335Hz, f_d=15.745Hz, f_m=15.567Hz

(d) No.4: f_p=0.345Hz, f_d=16.215Hz, f_m=15.790Hz

(d) No.5: f_p=0.372Hz, f_d=17.500Hz

(e) No.6: f_p=0.452Hz, f_d=21.244Hz, f_m=21.733Hz

Fig. 3 Natural frequencies and mode shapes of prototype and model

Before the commencement of the actual test under wind, the modal parameters of the assembled aeroelastic model of the full TV tower, including the natural frequencies, modal damping ratios and mode shapes, were carefully checked via tests of free decay vibration under initial excitation. Only miniature accelerometers were used in the test of modal checking. The

acceleration signals measured at four sections along the height were used to extract the natural frequencies and mode shapes through the traditional spectral analysis, and the damping ratios by using the logarithm decay method. Fig. 3 shows the comparison of the mode shapes and natural frequencies between the model and the prototype, where, the solid lines indicate the prototype mode shapes whilst the dash-dot lines and the solid squares represent the designed and measured mode shapes of the model, respectively. It can then be found that the vibrations of the TV tower are coupled in X and Y directions due to its asymmetry in both the stiffness and mass distributions.

Generally speaking, the natural frequencies and mode shapes of the prototype structure were well simulated on the aeroelastic model. The discrepancies in designed and measured natural frequencies (f_d and f_m) were less than 3% for the first four modes. However, the 5th mode was not identified on the model. The main reason was that the natural frequency and mode shape of the 5th mode were rather close to those of the 3rd mode according to the finite element computed results. This led to a difficulty to distinguish the two modes on the model. Furthermore, for the 6th mode (the first torsional mode), only the natural frequency was identified successfully, whilst its mode shape was not identified because the vibration of this mode was hardly excited out due to the too high torsional stiffness.

The damping ratios of the original model were very small (below 0.5%), therefore, a miniature mass damper (MD), a small mass lump supported with a thin nylon bar, was installed in the top segment of inner-layer coat to adjust the damping ratios of the modes of the entire structure vibration. The damping ratios of the modes dominated by the antenna mast vibration were adjusted via connecting softly some proper coast segments using adhesive paper-tapes. Through careful adjustments of the lump mass and the stiffness of the nylon bar of the miniature MD and of the number, locations and thickness of the soft connections between the mast model segments, the damping ratios were managed to increase to 1.7% and 1.9% for the 1st and 2nd modes (horizontal bending of the entire structure), 1.93% for the 6th mode (torsion of the main structure), 1.07% and 1.1% for the 3rd and 4th modes (dominated by horizontal bending of the antenna mast), respectively. The measured modal damping ratios well met to the design values, namely, 1.5~2.0% for the modes with significant vibration of the main structure and 1.0% for the modes dominated by the mast vibration, respectively. The above designed values of damping ratios had been determined according to the structural characteristics of the TV tower and the relevant codes in China (MCC 2002). It can thus conclude that the modal parameters of the TV tower were well modeled on the full tower aeroelastic model.

5. Simulation of wind field of atmospheric boundary layer

The target profiles of mean wind and turbulent intensity are as follows

$$U(Z) = U_G \left(Z/Z_G \right)^{\alpha} \tag{1}$$

$$I_u(Z) = 0.1(Z/Z_G)^{-\alpha-0.05} \tag{2}$$

where the terrain of Type C should be considered for the TV tower according to the Chinese Load Code for the Design of Building Structures (MCC 2002). Therefore, the exponent α is equal to 0.22 and the gradient height Z_G is equal to 400 m and 1.504 m for the prototype and model, respectively. The formula for the turbulent intensity comes from the literature (AIJ 1995) and was

required by the designing company and the owner. The required turbulent intensity of the longitudinal fluctuating velocity (u) at the gradient height reaches 10%. Thus, a set of passive devices (see Fig. 4) compounded of two spirelets at the upwind section 8.67 m from the turntable center, a grid of vertical bars at the upwind section 4.77 m from the turntable center, and 14-row small roughness blocks of 7.5 cm wide ×6.0 cm high×4.5 thick staggered with a central distance of 0.5 m, was used to simulate the wind field of atmospheric boundary layer. Fig. 5 shows the comparisons between the simulated and required profiles of mean wind and turbulent intensities. Fig. 6 shows those of turbulent spectra. It can then be seen that the simulated wind field was satisfied.

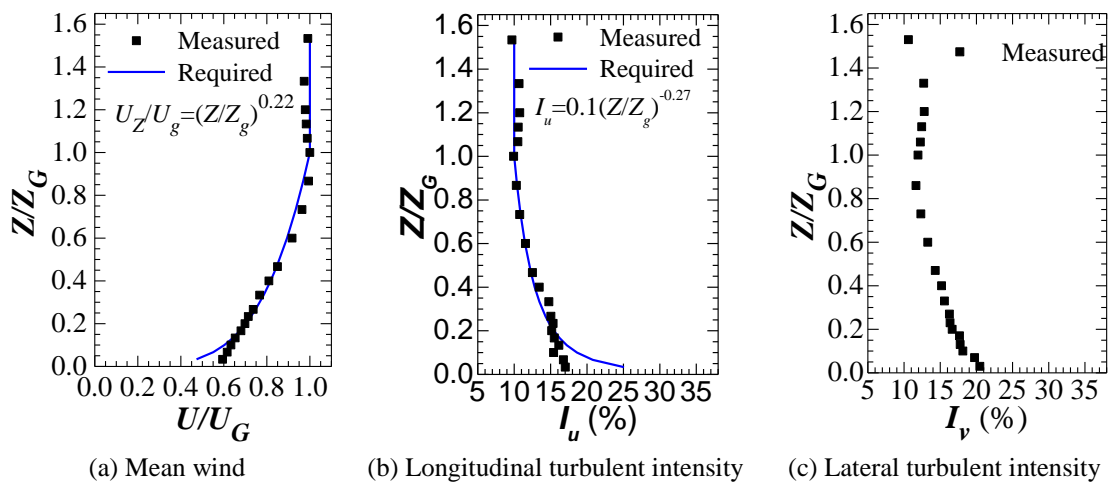Fig. 4 Passive devices for simulating wind field of atmospheric boundary layer

(a) Mean wind   (b) Longitudinal turbulent intensity   (c) Lateral turbulent intensity

Fig. 5 Profiles of mean wind and turbulent intensities

(a) Longitudinal component *u*

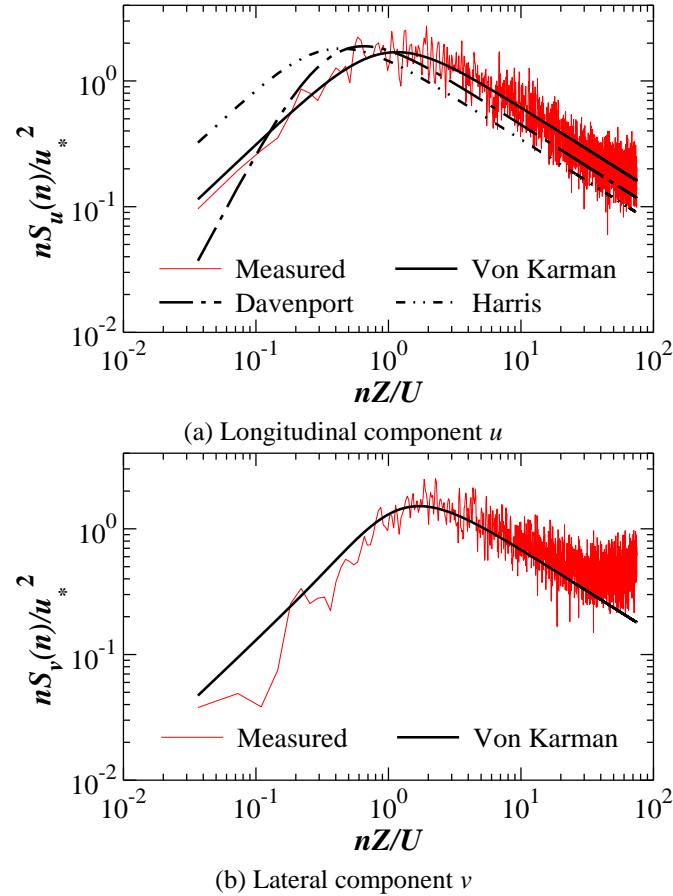
(b) Lateral component *v*

Fig. 6 Turbulence spectra at the top level of the main structure

6. Measurement sections and sensors

Because of the complexity of the appearance of the TV tower and the porosity of its outer frame canister, the selection of the installation positions for accelerometers and laser sensor targets was not freely, but constrained to some extent. Namely, some optimal positions on the model surface as desired were not proper for the instrument installation. Therefore, the principle of easy operation and reliable installation was adopted in the test. Hence, the elevations of some measurement sections and the positions of sensors and targets had to be adjusted slightly to meet the principle, leading to irregular installation positions. Finally, four measurement sections (MSs) were arranged on the aeroelastic model of the TV tower for measuring the responses of the tower model to turbulent wind in the wind tunnel test and to the initial excitations in free decay vibration test for the modal check before the wind tunnel test. As shown in Fig. 1(b), these measurement sections were numbered upwardly, and the corresponding prototype elevations of MS1 to MS4 were 278 m, 355 m, 443 m and 570 m, respectively. Thus, there were three measurement sections (MS1 to MS3) on the main structure and one measurement section (MS4) on the antenna mast.

For the main structure of the TV tower, three 1D laser displacement sensors and three 1D miniature accelerometers were mounted for each section of MS1 and MS3 to measure the horizontal translation displacements and accelerations in X (east) and Y (north) directions (see Fig. 1(c)) and the twist displacements and accelerations around the vertical axis Z at the elevations of 278 m and 443 m. Additionally, three 1D miniature accelerometers were installed on MS2 to measure the horizontal translation accelerations and the twist acceleration at the elevation of 355 m. To get the horizontal translation responses R_X and R_Y and the twist response $R_{\theta Z}$ of each section, the directly measured responses by the sensors (r_1, r_2 and r_3 as shown in Fig. 7) should be transformed using the following expression

$$\begin{Bmatrix} R_X \\ R_Y \\ R_{\theta Z} \end{Bmatrix} = \begin{bmatrix} \cos\alpha_1 & \sin\alpha_1 & x_1\sin\alpha_1 - y_1\cos\alpha_1 \\ \cos\alpha_2 & \sin\alpha_2 & x_2\sin\alpha_2 - y_2\cos\alpha_2 \\ \cos\alpha_3 & \sin\alpha_3 & x_3\sin\alpha_3 - y_3\cos\alpha_3 \end{bmatrix}^{-1} \begin{Bmatrix} r_1 \\ r_2 \\ r_3 \end{Bmatrix} \tag{3}$$

where the definitions of α_i, x_i, y_i are shown in Fig. 7, and R could be the displacement response or the acceleration response.

For the antenna mast, no laser displacement sensor was used for the displacement measurement because the dimension of the mast model was too small to install laser targets, and the twist response was also not interesting for the same reason. Therefore only two 1D miniature accelerometers, one in X direction and another in Y direction, were mounted on MS4 to measure horizontal translation accelerations of antenna mast at 570 m.
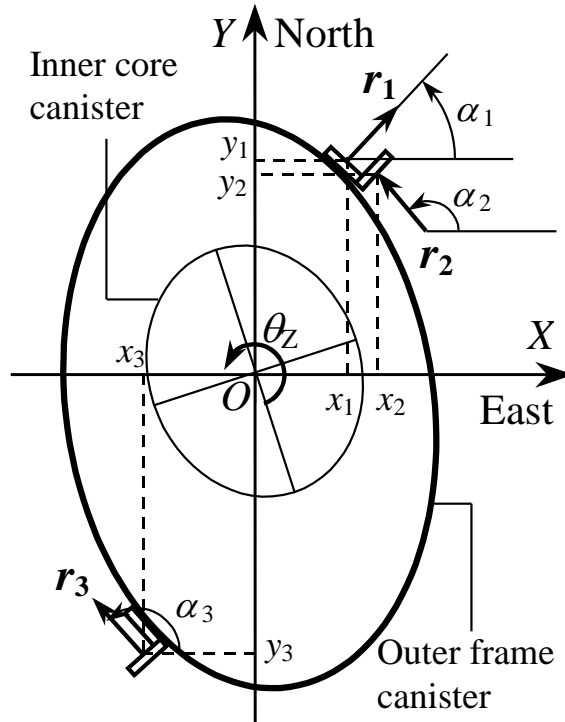

Fig. 7 Schematic diagram of the sensor positions and directions on a measurement section

7. Wind tunnel test and major results

The wind tunnel test of aeroelastic model was carried out for 32 wind directions (β) from 0° (due north) to 348.75° in clockwise at an interval of 11.25°. The design values of gradient wind speeds for 100-year and 10-year return periods are 52.4 m/s and 36.0 m/s, respectively, corresponding to 9.26 m/s and 6.36 m/s at the height of 1.504 m in the wind tunnel.

The reference point, used to monitor the test reference wind speed using a pitot-static tube, was set at the location about 1 m upwind from the center of turntable and 1.8 m above the wind tunnel floor (about 10 cm higher than the top of the main structure) to avoid significant disturbance due to the main structure. The reference test wind speed increased from 0 to 11 m/s at an interval of 1.0 or 1.5 m/s. Because the mean wind profile was well simulated (see Fig. 5(a)), the gradient wind speed was then monitored properly. The corresponding prototype wind speed was thus between 0.0 and 62.3 m/s, and the corresponding prototype reference height was 478.8 m.

No vortex-excited resonance phenomenon was observed in the test for all wind directions and wind speeds. Therefore, the following discussion will focus on the stochastic vibration responses of the TV tower to the turbulent wind.

7.1 Spectral responses

Fig. 8 shows some examples of response spectra, where, U_X, U_Y and R_{θ_z} are horizontal translation displacements along the axes of X and Y and the rotation angle around the axis of Z, respectively; a_X, a_Y and a_{θ_z} are horizontal translation accelerations along the axes of X and Y and the angular acceleration around the axis of Z, respectively, It can be found that the wind-induced vibration of the TV tower is coupled by multi-modes, but the several lower modes provide dominant contributions. The multi-mode coupling effect is more significant on the acceleration responses than on the displacement responses. For the main structure, the 1st mode provides the major contribution to the horizontal displacement and acceleration responses while the 2nd mode exerts a certain influence on them, and the contributions of other modes are small.

For the antenna mast, the contributions of the 3rd and 4th modes to the acceleration response are dominant, and about 5~20 times of that of the 1st mode in spectral amplitude, respectively. Considering that the natural frequencies of the 3rd and 4th modes are about 3.5 times of the 1st one, it can then be inferred in light of the stochastic theory that the contributions of the 3rd or 4th modes to the spectral responses of the mast displacements are only 1/7.5~1/30 of that of the 1st mode, and thus can be negligible obviously. Furthermore, the torsional responses were rather small compared with the horizontal responses.

7.2 Displacement responses

Because of the limitation of the testing condition, only the displacement responses at four measurement sections mentioned foregoing were directly measured in the test. However, the displacement responses at all structural floors are often needed in structural design to check the relative displacements between two adjacent floors. In this connection, the following least square approach is then presented to estimate indirectly the displacement responses of arbitrary floors based on the measured ones. In the light of the finite element method, a high-rise structure can be discretized into a *n*-DOF model of tandem lump masses as shown in Fig. 9, and the governing

equation of motion can be expressed as follows

$$\mathbf{M}\ddot{\mathbf{X}}_n(t) + \mathbf{C}\dot{\mathbf{X}}_n(t) + \mathbf{K}\mathbf{X}_n(t) = \mathbf{F}(t) \tag{4}$$

where $\mathbf{X}_n(t)$ is the vector of the displacement responses; $\mathbf{M, C}$ and $\mathbf{K}$ are the matrices of mass, damping and stiffness; $\mathbf{F}(t)$ is the loading vector. By using the modal superposition approach, the response can be approximately expressed with the modal displacement responses $\mathbf{q}_m(t) = (\mathbf{q}_1,\ldots,\mathbf{q}_m)^{\mathrm{T}}$ of m major modes as follows

$$\mathbf{X}_n(t) = \mathbf{\Phi}_{n\times m}\mathbf{q}_m(t) \tag{5}$$

where $\mathbf{\Phi}_{n\times m}$ is the matrix of mode shapes.

Let's denote $\hat{\mathbf{X}}_l(t)$ as the l-element vector of the measured displacement responses ($l \geq m$), the least square solution of the modal displacement response vector $\hat{\mathbf{q}}_m(t)$ can then be determined as follows

$$\mathbf{\Phi}_{l\times m}^{\mathrm{T}}\mathbf{\Phi}_{l\times m}\hat{\mathbf{q}}_m(t) = \mathbf{\Phi}_{l\times m}^{\mathrm{T}}\hat{\mathbf{X}}_l(t) \tag{6}$$

$$\hat{\mathbf{X}}_n(t) = \mathbf{\Phi}_{n\times m}\hat{\mathbf{q}}_m(t) \tag{7}$$

Furthermore, one can get the vector of standard deviation values ($\mathbf{\sigma}_{\hat{\mathbf{X}}_n}$) of the structural responses with statistic method based on the obtained time series of the responses $\hat{\mathbf{X}}_n(t)$, and the vector of peak values $\hat{\mathbf{X}}_{n\mathrm{Peak}}$ can be calculated by Eq. (8)

$$\hat{\mathbf{X}}_{n\mathrm{Peak}} = g_d\mathbf{\sigma}_{\hat{\mathbf{X}}_n} \tag{8}$$

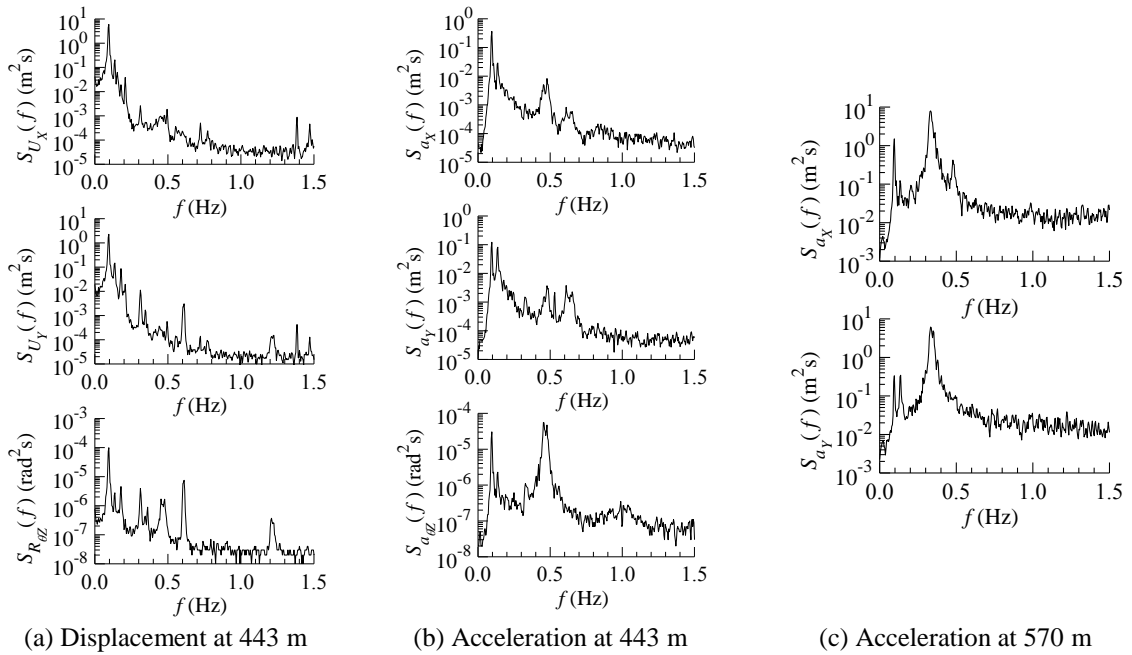(a) Displacement at 443 m   (b) Acceleration at 443 m   (c) Acceleration at 570 m

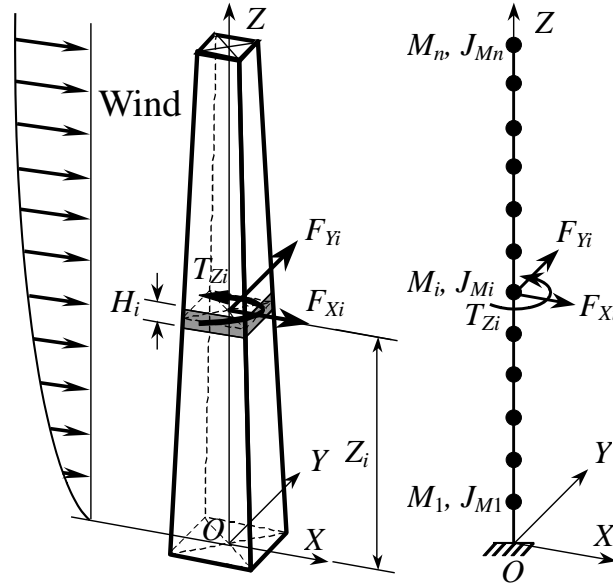Fig. 8 Response spectra (β=56.25°, U_G=53.9 m/s)

Fig. 9 Tandem lump mass model

where g_d is the peak factor of displacement responses, and is often set as 2.5~3.5.

Fig. 10 shows the variation curves of the mean and peak values of displacement responses of the main structure at the elevation of 443 m with the wind direction, where the gradient wind speed is 53.9 m/s. The horizontal responses vary approximately at a manner similar to sinusoid with the wind direction. The torsional responses are relatively small. Table 1 is a summary of the responses at the elevation of 443 m. It is seen that the absolute maximum of the peak displacement at the top of main structure in the X direction is 1.315 m and occurs at the wind direction of 56.25°. That in the Y direction reaches 0.914 m and occurs at the wind direction of 236.25°.

Table 1 Summary of responses at 443 m (U_G=53.9 m/s)

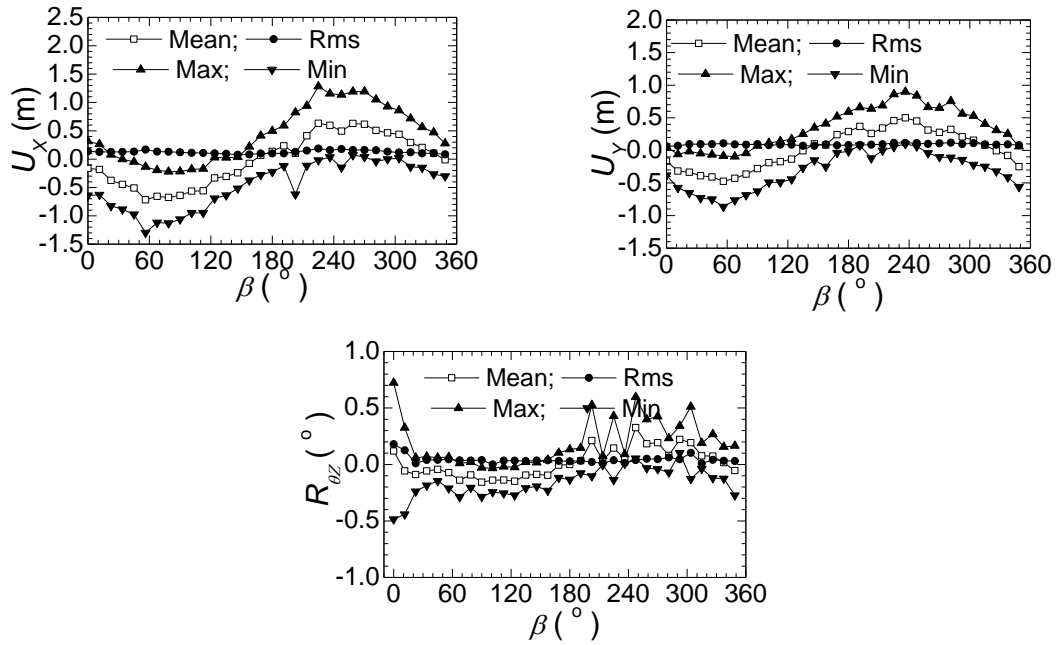| Response	U_X		U_Y		$R_{\theta Z}$		U_{farest}	
	β.(°)	Dis.(m)	β.(°)	Dis.(m)	β.(°)	Ang.(rad)	β.(°)	Dis.(m)
Max. mean displacement	225.00	0.638	236.25	0.513	292.50	0.00538	56.25	0.920
Min. mean displacement	56.25	-0.729	56.25	-0.478	112.50	-0.00332	337.50	0.164
Max. rms displacement	225.00	0.186	281.25	0.119	0.00	0.00313	225.00	0.219
Max. total displacement	56.25	1.315	236.25	0.914	0.00	0.01376	56.25	1.621

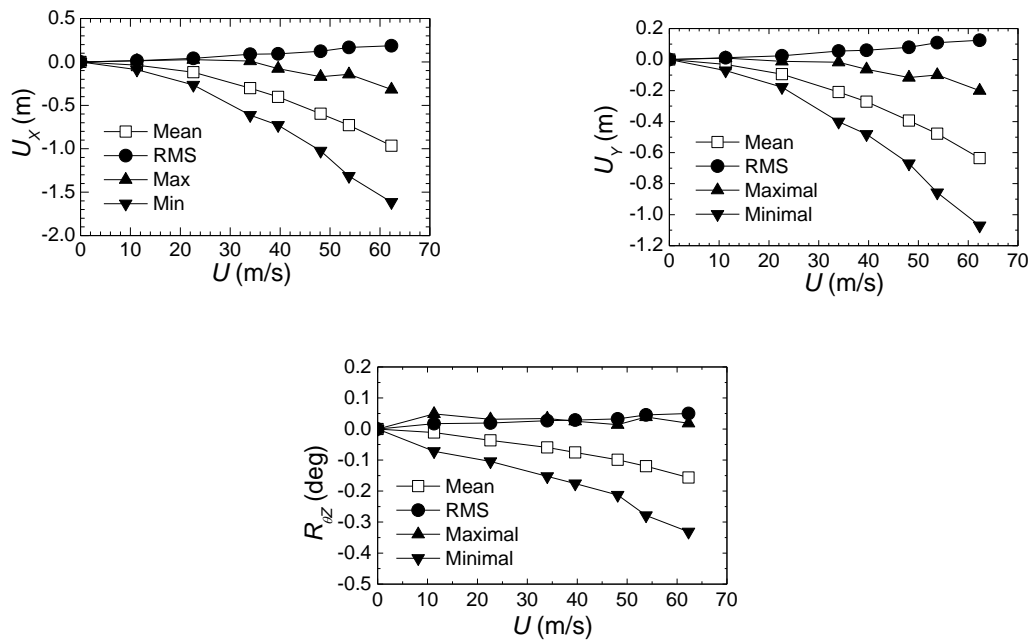Fig. 10 Displacement responses at 443 m vs. wind direction (U_G=53.9 m/s)

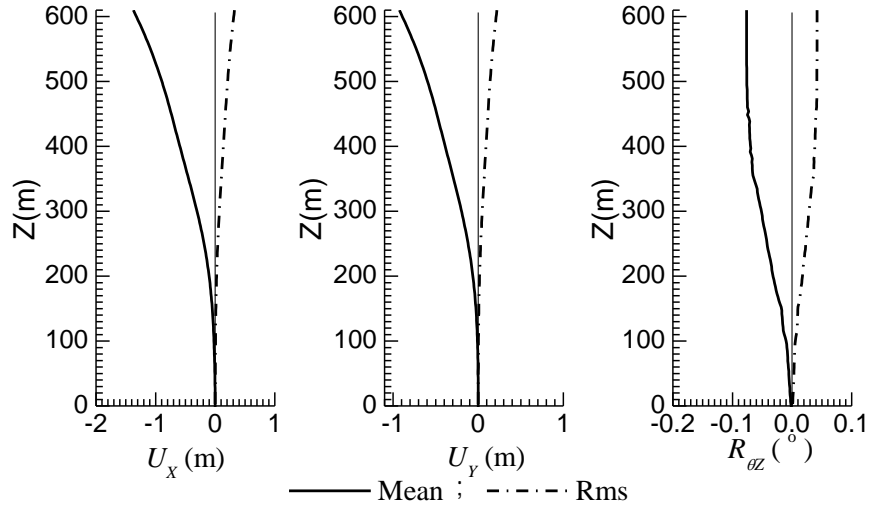Fig. 11 Displacement responses at 443 m vs. gradient wind speed (β=56.25°)

Fig. 12 Displacement responses vs. height (U=53.9 m/s, β=56.25°)

Fig. 11 shows the variation curves of displacements (mean, maximum and minimum responses) at the height of 443 m with the gradient wind speed for the wind direction of 56.25°. It can be seen that the horizontal responses vary approximately at quadric curves with the wind speed. The displacement responses at arbitrary structural floors could be indirectly estimated based on the measured ones using the foregoing-mentioned least square approach. Fig. 12 shows the mean and RMS displacement responses along the height, where the gradient wind speed is also 53.9 m/s and the wind direction is 56.25°.

7.3 Acceleration responses

Similarly, the least square solutions of the acceleration responses are as follows

$$\mathbf{\Phi}_{l\times m}^{\mathrm{T}}\mathbf{\Phi}_{l\times m}\hat{\ddot{\mathbf{q}}}_m(t) = \mathbf{\Phi}_{l\times m}^{\mathrm{T}}\hat{\ddot{\mathbf{X}}}_l(t) \tag{9}$$

$$\hat{\ddot{\mathbf{X}}}_n(t) = \mathbf{\Phi}_{n\times m}\hat{\ddot{\mathbf{q}}}_m(t) \tag{10}$$

$$\hat{\ddot{\mathbf{X}}}_{n\mathrm{Peak}} = g_a\mathbf{\sigma}_{\hat{\ddot{\mathbf{X}}}_n} \tag{11}$$

where g_a is the peak factor of acceleration responses, and often takes the value of 3.5~4.0.

Fig. 13 shows the variation curves of the RMS values of acceleration responses of the main structure at the height of 443 m and the mast at the height of 570 m versus the wind direction, where the gradient wind speed is also 53.9 m/s. Table 2 is a summary of the acceleration responses at the elevation of 443 m and 570 m. It is noted that the RMS value of the acceleration at the top of main structure in the X direction is 0.0614 m/s^2 and occurs at the wind direction of 270.0°. That in the Y direction reaches 0.0465 m/s^2 and also occurs at the wind direction of 270.0°.
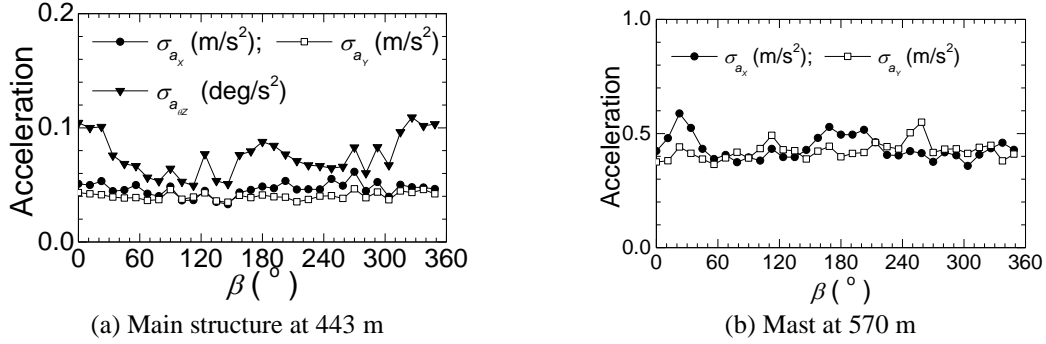
(a) Main structure at 443 m

(b) Mast at 570 m

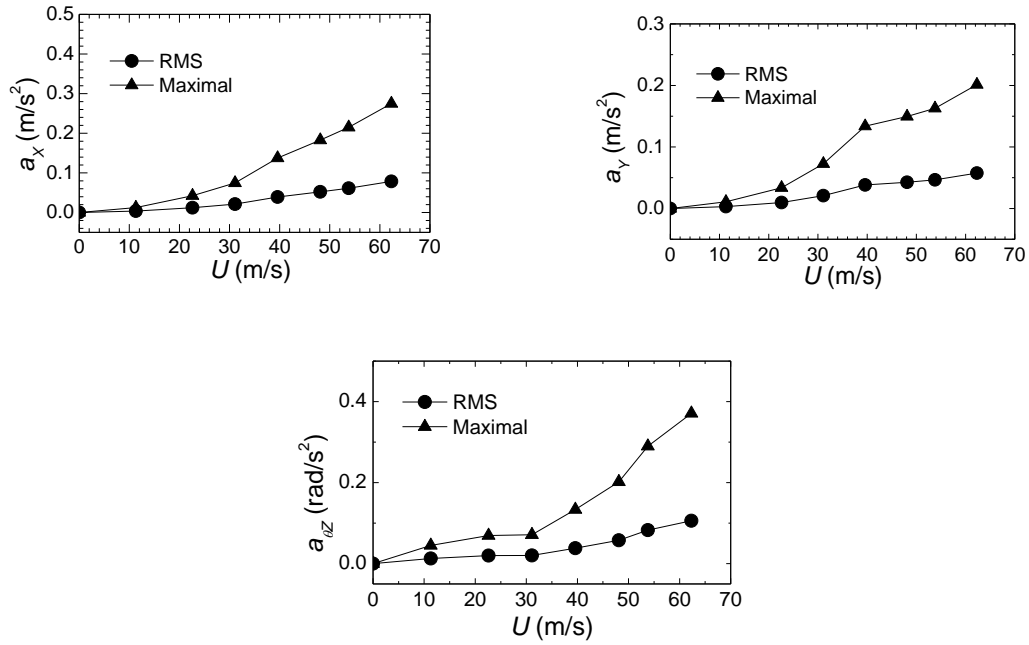Fig. 13 Acceleration responses vs. wind direction (U_G=53.9 m/s)

Fig. 14 Acceleration responses at 443m vs. gradient wind speed (β=270.0°)

Fig. 14 shows the variation curves of the acceleration responses at the height of 443 m with the gradient wind speed for the wind direction of 270.0°. The acceleration responses at arbitrary structural floors could be indirectly estimated based on the measured ones by using the above approach. Fig. 15 shows the maximal and RMS acceleration responses along the height of tower, where, the gradient wind speed is 53.9m/s and the wind direction is 270.0°. It can be seen that the acceleration responses of the TV tower in the two horizontal directions under wind loads are remarkable while the torsional accelerations are small.
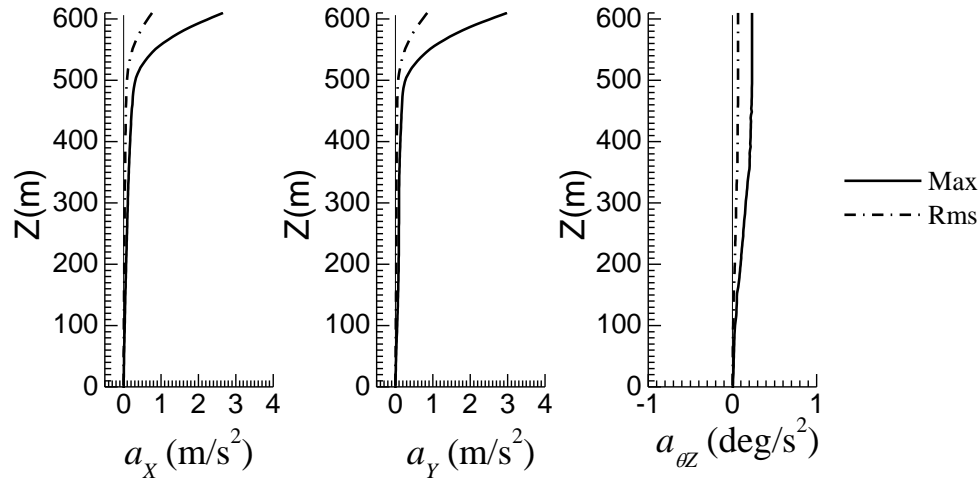
Fig. 15 Acceleration responses vs. height (U=53.9 m/s, β=270°)

Table 2 Summary of RMS values of acceleration responses (U_G=53.9 m/s)

Response	a_X		a_Y		$a_{\theta Z}$	
	$\beta.(°)$	Acel. (m/s²)	$\beta.(°)$	Acel. (m/s²)	$\beta.(°)$	Acel. (deg/s²)
Mast at 570m	22.50	0.5881	258.75	0.5496	-	-
Main structure at 443m	270.0	0.0614	270.0	0.0465	326.25	0.1092

8. Conclusions

In order to include the aeroelastic interaction between wind and structural motion, the aeroelastic model test of a 610 m-high TV tower with a complex and unique structural configuration and appearance was performed successfully. The aeroelastic model of the TV tower consisting of a steel core column with varying cross-section along the height, some divided coat segments and proper compensating weights, was designed to ensure the similarities of the major natural frequencies and the corresponding mode shapes. The modal parameters of the full tower, including the natural frequencies, modal damping ratios and mode shapes, were carefully checked using the approach of free decay vibration under initial excitation. It has been noted that the modal parameters of the TV tower were well modeled on the full tower model. Furthermore, the simulation of the atmospheric boundary layer with higher turbulent intensity is presented.

The major results show that the wind-induced vibration of this kind of TV tower is bi-directionally and multi-modally coupled and the dominant contributions from several lower modes. The multi-mode coupling effect is more significant on the acceleration responses than on the displacement responses.

Since the displacement and acceleration responses at several measurement sections were directly measured in the wind tunnel test, a multi-mode approach was presented to indirectly estimate the displacement and acceleration responses at arbitrary structural floors based on the measured ones. The horizontal displacement responses vary approximately at a manner similar to sinusoid with the wind direction and at quadric curves with wind speed. It can be seen that it is remarkable for the displacement and acceleration responses of the TV tower in the two horizontal directions under wind loads and is small for the dynamic response of the torsional displacement and acceleration.

Acknowledgments

References

Aly, A.M. (2013), "Pressure integration technique for predicting wind-induced response in high-rise buildings", *Alexandria Eng. J.*, **52**(4), 717-731.

Aly, A.M. (2014), "Atmospheric boundary-layer simulation for the built environment: past, present and future", *Build. Environ.*, **75**, 206-221.

Architectural Institute of Japan (AIJ), (1995), Recommendations for Loads on Building, Japan.

Baker, C.J. (2000), "Aspects of the use of proper orthogonal decomposition of surface pressure fields", *Wind Struct.*, **3**(2), 97-115.

Bienkiewicz, B., Tamura, Y., Ham, H.J., Ueda H. and Hibi, K. (1995), "Proper orthogonal decomposition and reconstruction of multi-channel roof pressure", *J. Wind Eng. Ind. Aerod.*, **54-55**, 369-382.

Boggs, D.W. and Peterka, J.A. (1989), "Aerodynamic model tests of tall buildings", *J. Eng. Mech. - ASCE*, **115**(3), 618-635.

Carassale, L., Piccardo, G. and Solari, G. (2001), "Double modal transformation and wind engineering applications", *J. Eng. Mech. - ASCE*, **127**, 432-439.

Davenport, A.G. (1961a), "A statistical approach to the treatment of wind loading on tall masts and suspension bridges", Ph.D Thesis, University of Bristol.

Davenport, A.G. (1961b), "The application of statistical concepts to the wind loading of structures", Proc. the Institute of Civil Engineers, London, UK, 19, 449-472.

Diana, G., Giappino, S., Resta, F., Tomasini, G. and Zasso, A. (2009), "Motion effects on the aerodynamic forces for an oscillating tower through wind tunnel tests", *Proceedings of the 5th European and African Conf. on Wind Engineering, Int. association for Wind Engineering*, EACWE 5: Florence, Italy.

Fediw, A.A., Nakayama, M., Cooper, K.R., Sasaki, Y., Resend, I.S. and Zan, S.J. (1995), "Wind tunnel study of an oscillating tall building", *J. Wind Eng. Ind. Aerod.*, **57**, 249-260.

Giappino, S., Rosa, L., Tomasini, G. and Zasso, A. (2015), "An aerodynamic and aeroelastic experimental study on a sectional and three-dimensional rectangular tall building", *Struct. Des. Tall Spec. Build.*, **25**, 139-157.

Gu, M. and Quan, Y. (2004), "Across-wind loads of typical tall buildings", *J. Wind Eng. Ind. Aerod.*, **92**(13), 1147-1165.

Kareem, A. (1992), "Dynamic response of high-rise buildings to stochastic wind loads", *J. Wind Eng. Ind. Aerod.*, **41-44**, 1101-1112.

Kikuchi, H., Tamura, Y., Ueda H. and Hibi, K. (1997), "Dynamic wind pressure acting on a tall building model-Proper orthogonal decomposition", *J. Wind Eng. Ind. Aerod.*, **69-71**, 631-646.

Kim, Y.M., You, K.P. and Ko, N.H. (2008), "Across-wind responses of an aeroelastic tapered tall building", *J. Wind Eng. Ind. Aerod.*, **96**, 1307-1319.

Kwok, K.C.S., (1982), "Cross-wind response of tall buildings", *Eng. Struct.*, **4**, 256-262.

Liang, S.G., Li, Q.S., Liu, S.C., Zhang, L.L. and Gu, M. (2004), "Torsional dynamic wind load on rectangular tall buildings", *Eng. Struct.*, **26**(1), 129-137.

Ministry of Construction P.R. China (MCC) (2002), Load Code for the Design of Building Structures, GB 50009-2001, China Architecture & Building Press.

Pozzuoli, C., Bartoli, G., Peil, U. and Clobes, M. (2013), "Serviceability wind risk assessment of tall buildings including aeroelastic effects", *J. Wind Eng. Ind. Aerod.*, **123**, 325-338.

Quan, Y. (1999), "Study on wind tunnel test of aeroelastic model of super-high-rise buildings", Master Thesis, Tongji University, China.

Rosa, L., Tomasini, G., Zasso, A. and Aly, A.M. (2012), "Wind-induced dynamics and loads in a prismatic slender building: A modal approach based on unsteady pressure measurements", *J. Wind Eng. Ind. Aerod.*, **107-108**, 118-130.

Solari, G. (1993), "Gust buffeting. II: dynamic alongwind response", *J. Struct. Eng.*, **119**, 383-398.

Tanaka, H., Tamura, Y., Ohtake, K., Nakai, M. and Kim. Y.C. (2012), "Experimental investigation of aerodynamic forces and wind pressures acting on tall buildings with various unconventional configurations", *J. Wind Eng. Ind. Aerod.*, **107-108**, 179-191.

Wang, F.Y. (1998), "Study on aerodynamic loads and wind effects of high-rise buildings using high-frequency force balance", Master Thesis, Tongji University, China.

Xu, Y.L. and Kowk, K.C.S. (1993), "Mode shape corrections for wind tunnel tests of tall buildings", *Eng. Struct.*, **15**, 387-392.

Ye, F. (2000), "Study on along-wind wind loads and responses of high-rise buildings", Master Thesis, Tongji University, China.

Zhou, Y., Gu M. and Xiang, H.F. (1999a), "Alongwind static equivalent wind loads and responses of tall buildings. Part II: Effects of mode shapes", *J. Wind Eng. Ind. Aerod.*, **79**, 151-158.

Zhou, Y., Gu, M. and Xiang, H.F. (1999b), "Alongwind static equivalent wind loads and responses of tall buildings. Part I: Unfavorable distributions of static equivalent wind loads", *J. Wind Eng. Ind. Aerod.*, **79**, 135-150.

Zhou, Y., Kareem, A. and Gu, M. (2000), "Equivalent static buffeting wind loads on structures", *J. Struct. Eng. - ASCE*, **126**, 989-992.

Zhou, Y., Kreeam A. and Gu M. (2002), "Mode shape corrections for wind load effects", *J. Eng. Mech. - ASCE*, **128**, 15-23.

CC